The Japan Society of Mechanical Engineers

Analysis of Negative Poisson's Ratios of Re-Entrant Honeycombs*

Hideyuki OHTAKI**, Guoming HU**, Yasumi NAGASAKA*** and Sinya KOTOSAKA**

Materials or structures that contract in the transverse direction under uniaxial compression, or expand laterally when stretched are said to have negative Poisson's ratios. A theoretical approach to the prediction of negative Poisson's ratios of re-entrant honeycombs has been developed which is based on the large deflection model. The equations of the deflection curves of the inclined member of the re-entrant cell, strains and Poisson's ratios of re-entrant honeycombs in two orthogonal directions have been derived. The deformed shapes of the inclined members of the re-entrant cell are calculated. The negative Poisson's ratios of re-entrant honeycombs are no longer a constant at large deformation. They vary significantly with the strain. The effect of the geometric parameters of the cell on the Poisson's ratios is analyzed.

Key Words: Bending, Nonlinear Problem, Flexible Structure, Boundary Conditions, Honeycomb, Poisson's Ratio, Deflection

1. Introduction

A negative Poisson's ratio has been treated as an abnormal elasticity for a long time. However, negative Poisson's ratios are theoretically permissible. For an isotropic material, the allowable range of Poisson's ratio is from −1.0 to 0.5, based on the thermodynamic consideration of strain energy in the theory of elasticity. Materials with naturally elaborated structures construction, like cancellous bone and rock with micro cracks, also have negative Poisson's ratios.

Fabrication of man-made materials and structures, which exhibit negative Poisson's ratios, has been successfully realized. Some examples are composite laminates, micro porous polymers, two-dimensional honeycombs and three-dimensional foams. Particularly, Lakes[1),(2)] had described a class of foams that constitute perhaps the only known isotropic materials with negative Poisson's ratios. Rothenburg et al.[3] proposed a general class of microstructure of isotropic materials that leads to negative Poisson's ratios.

All negative Poisson's ratio materials and structures are classified by Evans et al.[4] as auxetics or auxetic materials. Auxetic materials and their negative Poisson's ratios have not been well understood. Materials of this sort are expected to have interesting mechanical properties, such as high energy absorption, fracture toughness, indentation resistance and enhanced shear moduli, which may be useful in some applications. Here one can cite the works of Overaker et al.[5] and Wang and Cuitiño[6]. They studied the application of auxetic material to medical anchors and cushions. Therefore recently, the design and fabrication of auxetic materials and the analysis of their negative Poisson's ratios have simulated great interesting in the research community.

Saiki et al.[7] and Ohno et al.[8] applied the homogenization theory for periodic micro structures and realized mathematical consistency in characterizing macroscopic physical properties of heterogeneous media. Almgren[9], Wojciechowski and Branka[10),(11)] investigated theoretically by Monte Carlo method. Warren and coworkers[12),(13)] made an approach for analytically calculating the effective elastic properties of polymeric foams. Wei[14] presented a theoretical model for evaluating the effective Poisson's ratio of polymeric networks. Gibson and

* Received 23rd August, 2002 (No. 02-4153)

** Department of Mechanical Engineering, Faculty of Engineering, Saitama University, 255 Shimo-Okubo, Sakura-ku, Saitama 338–8570, Japan.
E-mail: ohtaki@post.saitama-u.ac.jp

*** Department of Mechanical Engineering, Faculty of Engineering, Nippon Institute of Technology, 4–1 Gakuendai, Miyashiro-machi, Minami-Saitama-gun, Saitama 345–8501, Japan

NII-Electronic Library Service

The Japan Society of Mechanical Engineers

Ashby[15] developed a model that successfully predicts Poisson's ratio for macroscopic honeycombs, assuming small deformation by flexure. Evans[16],[17] used a molecular mechanics program which incorporates a standard valence force field to model the deformation of network microstructure and thus to calculate Poisson's ratio. Warren and Byskov[18] studied the relationship of three fold symmetry and mechanical isotropy of two-dimensional materials based on a linear elastic micropolar model. The effects of structural geometric parameters on negative Poisson's ratio were investigated by Yang et al.[19] using a finite element method.

Sigmund[20],[21] reported that arbitrary materials can be obtained by modeling the base cell as a truss structure based on an inverse problem. Masters and Evans[22] showed that all materials exhibit negative Poisson's ratios as a result of their microstructures or geometric units. Honeycombs are considered as a basic structure of these microstructures or geometric units. An open cell in which the inclined members of the cell protrude inwards was described by Lakes[23] as a re-entrant cell. Making the cell of a conventional hexagonal honeycomb re-entrant produces a negative Poisson's ratio. This kind of honeycomb is described as auxetic honeycomb here. When honeycomb are to be used as load bearing or energy absorption structures, large deformation often occurs, and non linear behavior becomes important. This suggests that a large deformation model should be more appropriate. The in-plane buckling and non linear compression of conventional honeycombs had been analyzed by Zhang and Ashby[24], and Zhu and Mills[25] but these approaches either avoid the calculation of large deflection itself, or divide the deformed member into segments and calculate the large deflection by iteration. In this study, we limited our analysis to the negative Poisson's ratios of auxetic honeycombs, based on the large deflection model, and calculated the large deflection directly by incomplete elliptic integrals.

Nomenclature

E_s : Young's modulus of the solid cell member material
H : Length of the vertical cell member
I : Second moment of inertia of the cell member and $I=bt^3/12$
L : Length of the inclined cell member
L_{XX}, L_{YX} : Projected distances of the half inclined member along X-axis and Y-axis, respectively, under X-direction loading
L_{XY}, L_{YY} : Projected distances of the half inclined member along X-axis and Y-axis, respectively, under Y-direction loading
M_X, M_Y : Bending moments at the end of the inclined member due to σ_X and σ_Y, respectively
P_X, P_Y : Forces applied on the inclined member due to σ_X and σ_Y, respectively
R : Relative density of the re-entrant honeycomb
S : Distance of a general point along the curvilinear co-ordinates from origin O
b : Breadth of the cell member
k_X, k_Y : Square roots of ratio of P_X, P_Y to bending rigidity of the inclined member, respectively
p_X, p_Y : Equal to $\sin(\alpha_X/2)$ and $\sin(\alpha_Y/2)$, respectively
t : Thickness of the cell member
α_X, α_Y : Bending angles at origin O between the tangent of the inclined member and X-axis and Y-axis loading direction, respectively
β_X, β_Y : Bending angles at end B between the tangent of the inclined member and X-axis and Y-axis loading direction, respectively
γ : Bending angle at free end O of a horizontal cantilever beam predicted by small deformation of flexure
λ : Angle between the undeformed inclined member and X-axis
θ : Bending angle of a general point along a deformed member between the tangent of the shape of the inclined member and loading direction
ξ_X, ξ_Y : Upper limits of integrals for a general point along the half member with X-direction loading and Y-direction loading, respectively
δ_X, δ_Y : Lower limits of integrals with X-direction loading and Y-direction loading, respectively
ν : Poisson's ratio of solid material
ν_X, ν_Y : Poisson's ratios of the re-entrant honeycomb under X-direction loading and Y-direction loading, respectively
ϕ : New integral variable
ε : Strain of honeycomb
ε_{XX}, ε_{YX} : Strains of the honeycomb in X-direction and Y-direction, respectively ,due to σ_X
ε_{XY}, ε_{YY} : Strains of the honeycomb in X-direction and Y-direction, respectively, due to σ_Y
ρ : Density of the re-entrant honeycomb
ρ_S : Density of the solid cell material
σ_X, σ_Y : Remote stresses applied on the re-entrant honeycomb in X-direction and Y-direction, respectively

2. Analysis of Negative Poisson's Ratios of Re-Entrant Honeycombs by Large Deflection Model

2.1 Forces and moments on the cell members

For a re-entrant honeycomb as shown in Fig. 1, assuming that re-entrant cells have uniform thickness, and that t/L is small, the relative density giving by simple geometry is:

$$R=\frac{\rho}{\rho_S}=\frac{t/L(H/L+2)}{2\cos\lambda(H/L-\sin\lambda)} \tag{1}$$

When the re-entrant honeycomb is uniaxially loaded in the X or Y direction as shown in Fig. 2, the re-entrant

NII-Electronic Library Service

The Japan Society of Mechanical Engineers

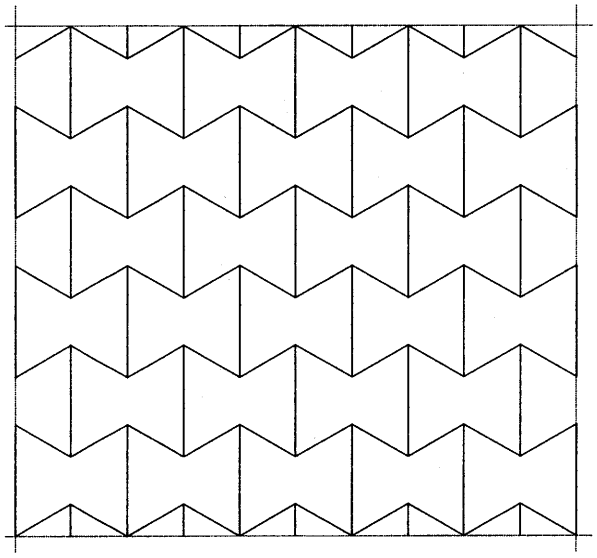

Fig. 1 An undeformed auxetic honeycomb with re-entrant cells

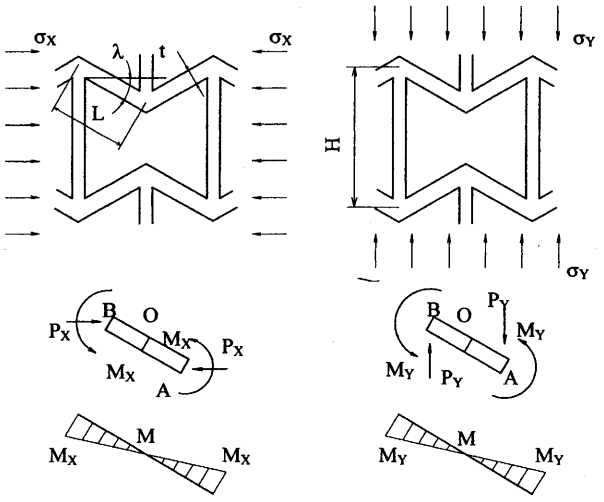

(a) Loaded in X-direction (b) Loaded in Y-direction

Fig. 2 Cell deformation by inclined cell member bending

cell members bend. The remote stress σ_X or σ_Y produces force P_X or P_Y on inclined members of a unit cell, parallel to the X-axis or the Y-axis. P_X and P_Y are given by:

$$P_X = \sigma_X (H - L\sin\lambda) b \tag{2}$$

$$P_Y = \sigma_Y L\cos\alpha b \tag{3}$$

By equilibrium of the moment, the bending moments at the end of the inclined member are:

$$M_X = P_X L\sin\lambda/2 \tag{4}$$

$$M_Y = P_Y L\cos\lambda/2 \tag{5}$$

2.2 Large deflection model

As can be seen from Fig. 2, there is a zero bending moment at the midpoint of the inclined member. Thus only the deformation shape of the half member will be analyzed. The moment distribution in OB is the same as if it were a cantilever beam, loaded at the free end by force P_X

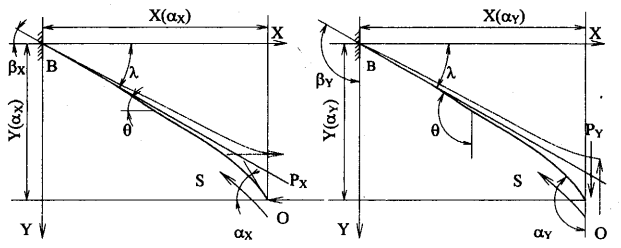

(a) Loaded in X-direction (b) Loaded in Y-direction

Fig. 3 Large deflection model of the half inclined member (The solid line represents the deformation caused by a remote compressive stress, while the dashed line represents the deformation caused by a remote tensil stress)

acting in the X-direction (see Fig. 3 (a)). A curvilinear coordinate S, with origin O, is used to define position in the bending member. The exact expression for the curvature of OB is $d\theta/dS$. Since the bending moment in OB is equal to the flexural rigidity times the curvature, the differential equation of the deflection curve is:

$$E_S I\frac{d\theta}{dS} = -P_X Y \tag{6}$$

and the boundary conditions are:

$$\left(E_S I\frac{d\theta}{dS}\right)_{s=0} = 0, \quad (\theta)_{s=0} = \alpha_X \tag{7}$$

$$\left(E_S I\frac{d\theta}{dS}\right)_{s=L/2} = M_X, \quad (\theta)_{s=L/2} = \beta_X \tag{8}$$

Neglecting the change in length of OB due to axial compression, differentiating Eq. (6) with respect to S, and using the relation $dY/dS = \sin\theta$ we obtain:

$$E_S I\frac{d^2\theta}{dS^2} = -P_X\sin\theta \tag{9}$$

In solving Eq. (9), we begin by multiplying both sides by $\frac{d\theta}{dS}dS$ and integrating, so that:

$$\int \frac{d^2\theta}{dS^2}\frac{d\theta}{dS} = -k_X^2\int \sin\theta\frac{d\theta}{dS}dS \tag{10}$$

where $k_X^2 = \frac{P_X}{E_S I}$. Upon integrating, and using the boundary condition at O, we obtain:

$$\left(\frac{d\theta}{dS}\right)^2 = 2k_X^2(\cos\theta - \cos\alpha_X) \tag{11}$$

It can be seen from Fig. 3 (a) that $d\theta/dS$ is always negative, and thus solving for dS gives:

$$dS = -\frac{d\theta}{k_X\sqrt{2(\cos\theta - \cos\alpha_X)}} \tag{12}$$

The total length of the half member, after the limits of integration are interchanged, is:

$$\frac{L}{2} = \int_{\beta_X}^{\alpha_X}\frac{d\theta}{k_X\sqrt{2(\cos\theta - \cos\alpha_X)}} = \frac{1}{2k_X}\int_{\beta_X}^{\alpha_X}\frac{d\theta}{\sqrt{\sin^2(\alpha_X/2) - \sin(\theta/2)}} \tag{13}$$

NII-Electronic Library Service

The Japan Society of Mechanical Engineers

Using the notation $p_X = \sin(\alpha_X/2)$ and by introducing a new variable ϕ in such a manner that:

$$\sin(\theta/2) = p_X \sin\phi = \sin(\alpha_X/2)\sin\phi \tag{14}$$

it is seen from this relation that the limits of integration in the θ-coordinates $\theta = \alpha_X$ and $\theta = \beta_X$ transform into that in the ϕ-coordinates, and thus are

$$\phi|_{\theta=\alpha_X} = \pi/2$$

and

$$\phi|_{\theta=\beta_X} = \delta_X = \arcsin\left(\sin\frac{\beta_X}{2} \Big/ \sin\frac{\alpha_X}{2}\right) \tag{15}$$

Differentiating Eq. (14) gives:

$$d\theta = \frac{2p_X \cos\phi d\phi}{\sqrt{1-p_X^2\sin^2\phi}} \tag{16}$$

Substituting Eqs. (14), (16) into Eq. (13), we obtain:

$$L = \frac{2}{k_X}\int_{\delta_X}^{\pi/2} \frac{d\phi}{\sqrt{1-p_X^2\sin^2\phi}} = \frac{2}{k_X}F(\alpha_X) \tag{17}$$

where $F(\alpha_X)$ is an incomplete elliptic integral of the first kind, and its value depends on the inclinations α_X and β_X of the points O and B. The force P_X is related to this elliptic integral by:

$$P_X = k_X^2 E_S I = \frac{4E_S I F^2(\alpha_X)}{L^2} \tag{18}$$

When the re-entrant honeycomb is uniaxially loaded in the Y-direction (see Fig. 3 (b)), P_Y can be obtained by the same procedure as the solution for P_X, and is expressed as:

$$P_Y = k_Y^2 E_S I = \frac{4E_S I F^2(\alpha_Y)}{L^2} \tag{19}$$

$$F(\alpha_Y) = \int_{\delta_Y}^{\pi/2} \frac{d\phi}{\sqrt{1-p_Y^2\sin^2\phi}}$$

In the above equation, the incomplete integral $F(\alpha_Y)$ is related to two parameters:

$$p_Y = \sin(\alpha_Y/2)$$

and

$$\delta_Y = \arcsin\left(\sin\frac{\beta_Y}{2} \Big/ \sin\frac{\alpha_Y}{2}\right) \tag{20}$$

For a given value of α_X or α_Y, P_X or P_Y can be calculated through these incomplete elliptic integrals. It should be noted that in the re-entrant cell (see Fig. 4), the direction of the forces in the inclined members is reversed in contrast with that in the inclined members of a conventional hexagonal cell, while the forces in the vertical members remain unchanged.

2.3 Strain and Poisson's ratio for loading in the X-direction

The horizontal projection dL_{XX} of the element dS of the half member OB is $dS\cos\theta$ when the auxetic honeycomb bears a remote tensile stress, and is $dS\cos\theta$ when the auxetic honeycomb bears a remote compressive stress. So the horizontal projected distance $L_{XX}(\theta)$ of a general point on the half member along the X-axis due to X-direction loading is:

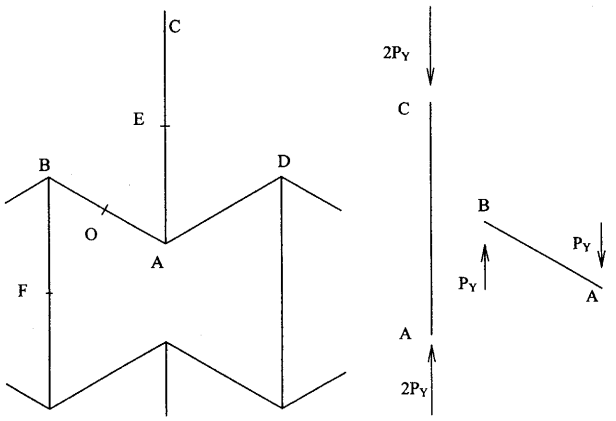

Fig. 4 An re-entrant cell unit formed by triangular prisms

$$L_{XX}(\theta) = \frac{1}{2k_X}\int_{\beta_X}^{\theta} \frac{\pm\cos\theta d\theta}{\sqrt{\sin^2(\alpha_X/2)-\sin^2(\theta/2)}} \tag{21}$$

Writing $\cos\theta$ as $1-2\sin^2(\theta/2)$ and using Eqs. (14) and (16), the above equation can be expressed in terms of ϕ:

$$L_{XX} = \frac{\pm 1}{k_X}\int_{\delta_X}^{\xi_X} \frac{1-2p_X^2\sin^2\phi}{\sqrt{1-p_X^2\sin^2\phi}}d\theta$$

$$= \frac{\pm 1}{k_X}\left[2\int_{\delta_X}^{\xi_X}\sqrt{1-p_X^2\sin^2\phi}\,d\phi - \int_{\delta_X}^{\xi_X}\frac{1}{\sqrt{1-p_X^2\sin^2\phi}}d\theta\right] \tag{22}$$

where $\xi_X = \arcsin\left(\sin\frac{\theta}{2} \Big/ \sin\frac{\alpha_X}{2}\right)$ and $\beta_X \le \theta \le \alpha_X$.

The first part of the right-hand side of this equation is an incomplete elliptic integral of the second kind, and can be designated as $E(\xi_X)$, so the horizontal projected distance is:

$$L_{XX}(\theta) = \frac{\pm 1}{k_X}[2E(\xi) - F(\xi)] \tag{23}$$

Letting the upper limit of the integration be $\pi/2$, the total projected length of the half member OB along the X-axis due to X-direction loading is:

$$L_{XX}(\alpha_X) = \frac{\pm 1}{k_X}[2E(\alpha_X) - F(\alpha_X)] \tag{24}$$

As the horizontal length of the undeformed inclining member AB is $L\cos\lambda$ (see Fig. 4), the strain in the horizontal direction due to σ_X is:

$$\varepsilon_{XX} = \frac{2L_{XX}(\alpha_X) - L\cos\lambda}{L\cos\lambda}$$

$$= \frac{\pm 2[2E(\alpha_X) - F(\alpha_X)]/k_X - L\cos\lambda}{L\cos\lambda} \tag{25}$$

The vertical projected distance $L_{YX}(\theta)$ of a general point on the half member along the Y-axis can be calculated in a similar way, and is expressed as:

$$L_{YX}(\theta) = \frac{1}{2k_X}\int_{\beta_X}^{\theta} \frac{\sin\theta d\theta}{\sqrt{\sin^2(\alpha_X/2)-\sin^2(\theta/2)}} \tag{26}$$

As $\sin\theta = 2\sin(\theta/2)\cos(\theta/2) = 2\sin(\theta/2)(1-\sin^2(\theta/2))^{1/2}$, and expressing the above equation in terms

NII-Electronic Library Service

The Japan Society of Mechanical Engineers

of ϕ, we obtain:

$$L_{YX}(\theta)=\frac{2p_X}{k_X}\int_{\delta_X}^{\xi_X}\sin\phi d\phi=\frac{2p_X}{k_X}(\cos\delta_X-\cos\xi_X) \tag{27}$$

Letting $\xi_X=\pi/2$, the total projected length of the half member OB along the Y-axis is

$$L_{YX}(\alpha_X)=\frac{2p_X}{k_X}\cos\delta_X \tag{28}$$

The vertical lengths of the undeformed inclined member AB and the vertical half members AE and BF are $L\sin\lambda$ and H (see Fig. 4), respectively. The strain in the vertical direction depends on the total projected lengths of AB, AE and BF along the Y-axis. As vertical members do not deform in this large deflection model, the strain in the vertical direction due to σ_X is:

$$\varepsilon_{YX}=\frac{H-2L_{YX}(\alpha_X)-(H-L\sin\lambda)}{H-\lambda\sin\lambda}=\frac{L\sin\lambda-4p_X\cos\delta_X/k_X}{H-L\sin\lambda} \tag{29}$$

The Poisson ratio under X-direction loading is calculated as the negative transverse strain divided by the axial strain in the loading direction:

$$\nu_X=-\frac{\varepsilon_{YX}}{\varepsilon_{XX}}=-\frac{L\sin\lambda-4p_X\cos\delta_X/k_X}{H-L\sin\lambda}\Bigg/\frac{\pm2[2E(\alpha_X)-F(\alpha_X)]/k_X-L\cos\lambda}{L\cos\lambda} \tag{30}$$

2.4 Strain and Poisson's ratio for loading in the Y-direction

With a similar approach to that in the above subsection, we can calculate the projected distances of the deformed half member, and the strains along the horizontal and vertical directions, and therefore the Poisson's ratio for loading in the Y-direction. The solution for the horizontal projected length L_{XY} of the half member along the X-axis for this loading direction is similar to the solution of L_{YX}, instead of L_{XX}, with minor modification. The horizontal projected distance $L_{XY}(\theta)$ of a general point on the half member and the total horizontal projected length $L_{XY}(\alpha_Y)$ of the half member OB along the X-axis due to Y-direction loading are:

$$L_{YX}(\theta)=\frac{1}{2k_Y}\int_{\beta_Y}^{\theta}\frac{\sin\theta d\theta}{\sqrt{\sin^2(\alpha_Y/2)-\sin^2(\theta/2)}}=\frac{2p_Y}{k_Y}(\cos\delta_Y-\cos\xi_Y) \tag{31}$$

$$L_{XY}(\alpha_Y)=\frac{2p_Y}{k_Y}\cos\delta_Y \tag{32}$$

where $\xi_Y=\arcsin\left(\sin\frac{\theta}{2}\Big/\frac{\alpha_Y}{2}\right)$ and $\beta_Y\le\theta\le\alpha_Y$. Similarly, the vertical projected distance $L_{YY}(\theta)$ of a general point on the half member and the total vertical projected length $L_{YY}(\alpha_Y)$ of the half member OB along the Y-axis due to Y-direction loading are:

$$L_{YY}(\theta)=\frac{1}{2k_Y}\int_{\beta_Y}^{\theta}\frac{\pm\cos\theta d\theta}{\sqrt{\sin^2(\alpha_Y)-\sin^2(\theta/2)}}=\frac{\pm1}{k_Y}[2E(\xi_Y)-F(\xi_Y)] \tag{33}$$

$$L_{YY}(\alpha_Y)=\frac{\pm1}{k_Y}[2E(\alpha_Y)-F(\alpha_Y)] \tag{34}$$

where the positive sign indicates that the auxetic honeycomb undergoes a remote tensile stress, while the negative sign indicates that the auxetic honeycomb undergoes a remote compressive stress.

For loading in the Y-direction, the strains in the vertical direction and horizontal direction due to σ_Y are:

$$\varepsilon_{YY}=\frac{H-2L_{YY}(\alpha_Y)-(H-L\sin\lambda)}{H-L\sin\lambda}=\frac{L\sin\lambda\mp2[2E(\alpha_Y)-F(\alpha_Y)]/k_Y}{H-L\sin\lambda} \tag{35}$$

$$\varepsilon_{XY}=\frac{2L_{XY}(\alpha_Y)-L\cos\lambda}{L\cos\lambda}=\frac{4p_Y\cos\delta_Y/k_Y-L\cos\lambda}{L\cos\lambda} \tag{36}$$

Thus the Poisson ratio for loading in the Y-direction is

$$\nu_Y=-\frac{\varepsilon_{XY}}{\varepsilon_{YY}}=-\frac{4p_Y\cos\delta_Y/k_Y-L\cos\lambda}{L\cos\lambda}\Bigg/\frac{L\sin\lambda\mp2[2E(\alpha_Y)-F(\alpha_Y)]/k_Y}{H-L\sin\lambda} \tag{37}$$

3. Results and Discussion

3.1 Degeneration of the large deflection model

Referring back to Fig. 3 (b), letting $\lambda=\pi/2$, and considering that the half member OB is under remote compressive stress and that the deflection of OB is very small, the compressive force predicted by Eq. (19) is

NII-Electronic Library Service

The Japan Society of Mechanical Engineers

$$P_Y = \frac{\pi^2 E_S I}{4L^2} \tag{38}$$

which is the value of the critical load for the elastic buckling of a vertical bar as described by Timoshenko and Gere.

Let $\lambda = 0$, and consider that the half member OB undergoes a Y-direction force at point O. From Eq. (32), we have:

$$P_Y = E_S I \left(\frac{2p_Y \cos\delta_Y}{L_{XY}(\alpha_Y)} \right)^2 \tag{39}$$

When the deflection of OB is very small, we have: $\beta_Y = \pi/2$, $\alpha_Y = \pi/2 + \gamma$, and $L_{XY}(\alpha_Y) = L/2$. Through a set of mathematical processing steps, γ is expressed as

$$\begin{aligned} &\beta_Y = \pi/2, \quad \alpha_Y = \pi/2 + \gamma \\ &\gamma = -\frac{P_Y L^2}{8E_S I} \\ &L_{XY}(\alpha_Y) = L/2 \end{aligned} \tag{40}$$

which is the expression of the bending angle at end O of a cantilever beam fixed at end B and loaded at free end O by force P_Y, as predicted by the theory of the small deformation of flexure.

Therefore, this large deflection model also contains information of the elastic buckling and small deformation of flexure.

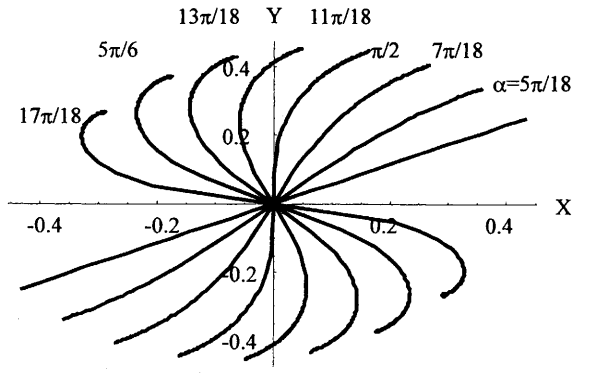

(a) Compressive loading

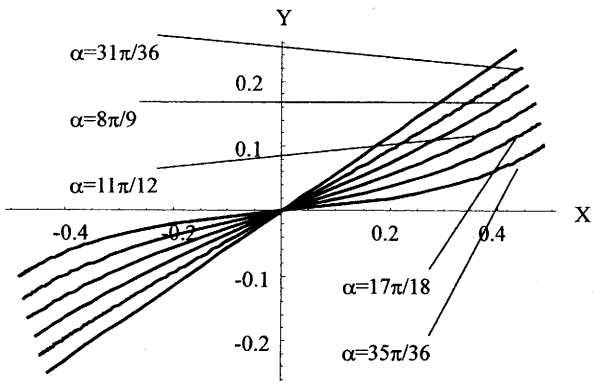

(b) Tensil loading

Fig. 5 Deformed shapes of an inclined member under X-direction loading with $H/L = 2$ and $\lambda = \pi/6$

3.2 The shape of the deformed member AB

Using Eqs. (23), (26), or (31), (33), the coordinates of a general point on the deflection member along the X-axis or the Y-axis can be calculated. The shape of the deformed member becomes S-shape. Setting the mid-point O as the origin, the shapes of the deflection curves for various values of α_X and α_Y are shown in Figs. 5 and 6, representing the compressive and tensile loading in the X-direction and Y-direction, respectively. In these figures, the cell's geometric parameters considered are: $H = 2L$, $\lambda = \pi/6$.

At compressive loading, the inclined members will touch each other, if the deformation is sufficiently large. At this time, the force and the moment distribution will change, which means that this large deflection model is not suitable for a higher deformation than the critical point of touch. The contact between the inclined members will not occur when the auxetic honeycomb is stretched.

3.3 Poisson's ratio versus strain

Poisson's ratios for X-direction loading and Y-direction loading are obtained from Eqs. (30) and (37), respectively. The Poisson's ratios ν_X and ν_Y for loading in the X-direction and the Y-direction are, as expected, independent of density, for the large deformation model used here neglects axial compression.

Figure 7 shows Poisson's ratios in the orthogonal directions versus strain for the case of $H = 2L$ and $\lambda = \pi/6$. It can be seen that Poisson's ratios are not constant, and

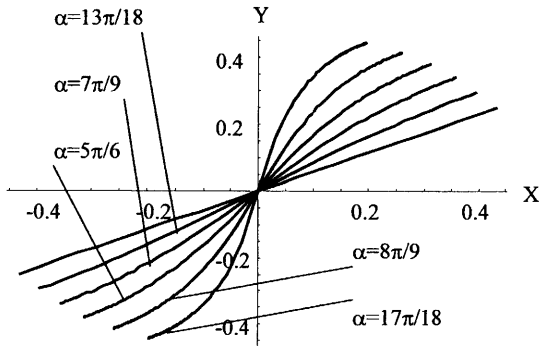

(a) Compressive loading

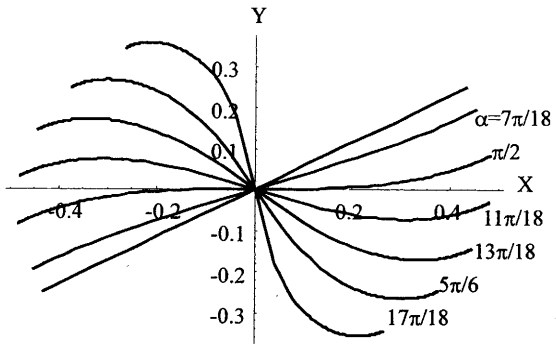

(b) Tensil loading

Fig. 6 Deformed shapes of an inclined member under Y-direction loading with $H/L = 2$ and $\lambda = \pi/6$

NII-Electronic Library Service

The Japan Society of Mechanical Engineers

are negative in general. The magnitude of Poisson's ratio decreases significantly at high strain when the auxetic honeycomb is compressed in X-direction loading or stretched in Y-direction loading, while if increases significantly at high strain when the auxetic honeycomb is stretched in X-direction loading or is compressed in Y-direction loading. Poisson's ratio at the limit value of small deformation is -1; the same result was obtained by Gibson et al.[15] and Masters and Evans[22].

The variation of Poisson's ratio versus strain is different for compressive loading and tensile loading at large deformation. For X-direction loading, the magnitude of Poisson's ratio decreases as strain increases when the auxetic honeycomb is compressed, and increases as strain increases when it is stretched. For Y-direction loading, Poisson's ratio becomes increasingly negative as strain increases when the auxetic honeycomb is compressed, and becomes decreasingly negative as strain increases when it is stretched. In particular, when the auxetic honeycomb undergoes a tensile stress in the Y-direction or undergoes a compressive stress in the X-direction at large deformation, the sign of Poisson's ratio may change from negative to positive. This phenomenon can be explained on the basis of Figs. 5 (a) and 6 (b). As can be seen from Fig. 6 (b), the horizontal projected length of member AB increases as α_Y, the bending angle at origin O, increases, when α_Y changes from $\pi/2-\lambda$ to $\pi/2$, but when α_Y exceeds $\pi/2$, it decreases as α_Y increases. In Fig. 5 (a), the vertical projected length of member AB increases as α_X increases when α_X changes from λ to $\pi/2$, but decreases as α_X increases when α_X changes from $\pi/2$ to π.

3.4 Effect of geometry on Poisson's ratio

To investigate the effect of geometry of the re-entrant cell on Poisson's ratio, ν_X and ν_Y at the limit of small deformation are tabulated in Tables 1 and 2 for the combinations of H/L and λ. In reality, the negative Poisson's ratios in the parentheses of these tables are never achieved, because for geometric considerations, the inclined members of the cells will touch each other before deformation with these geometric parameters of H/L and λ. ν_X and ν_Y, as they depends on the values of λ and H/L are also plotted in Figs. 8 and 9 for a given value of λ and for varying H/L, and for a given value of H/L and for varying λ, respectively.

As can be seen from Tables 1 and 2, negative Poisson's ratios at the limit of small strain converge to the result predicted by the small deformation of flexure:

$$\nu_X = -\frac{\cos^2\lambda}{(H/L-\sin\lambda)\sin\lambda} \tag{41}$$

$$\nu_Y = -\frac{(H/L-\sin\lambda)\sin\lambda}{\cos^2\lambda} \tag{42}$$

ν_X and ν_Y comply with the reciprocal relation $\nu_X\cdot\nu_Y=1$ for the same geometric parameters. In particular, the orthogonal symmetry of Poisson's ratio occurs for some cells with their geometric parameters satisfying:

$$\sin\lambda H/L=1 \tag{43}$$

and Poisson's ratio of this sort of auxetic honeycombs is minus one. A special case is the cell with geometric parameters of $H/L=2$ and $\lambda=\pi/6$. In contrast with the conventional regular hexagonal honeycomb, such cells have the same magnitude of Poisson's ratio, but with a different sign; and have the same inclination angle of the inclined member, but in a different direction. The relative density of this auxetic honeycomb calculated by Eq. (1) is larger than that of the conventional regular honeycomb. A re-entrant honeycomb with geometric parameters of $H/L=3$ and $\lambda=\pi/6$ has the same relative density as the conventional regular honeycomb, but their magnitudes of Poisson's ratios are different.

From Figs. 8 and 9, we know that Poisson's ratio not only varies significantly with the strain in all cases of geometric parameters, but is also influenced significantly by the geometric parameters of the cell. As H/L becomes large, the magnitude of ν_X reduces while the magnitude of ν_Y increases generally, for a given value of strain. A similar tendency occurs for the influence of λ on ν_X and ν_Y. The effect of H/L on ν_Y under tensile loading in the Y-direction becomes complicated when the deformation

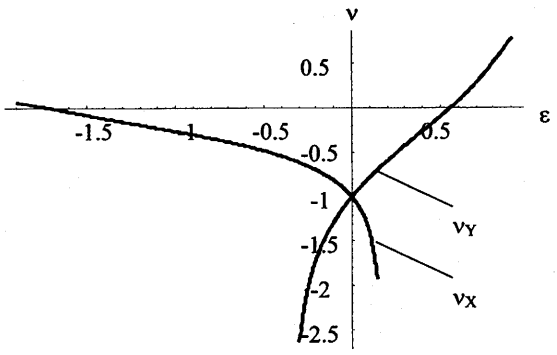

Fig. 7 Poisson's ratios vary with strain for a re-entrant cell with geometric parameters of $H/L=2$ and $\lambda=\pi/6$

Table 1 Poisson's ratio ν_X at the limit value of small deformation

	H/L	1.5	2	2.5	3	3.5	4
λ	π/18	-4.211	-3.058	-2.40	-1.976	-1.679	-1.460
	π/9	-2.230	-1.557	-1.196	-0.971	-0.818	-0.706
	π/6	-1.5	-1	-0.75	-0.6	-0.5	-0.429
	2π/9	-1.065	-0.673	-0.492	-0.387	-0.320	-0.272
	5π/18	(-0.735)	-0.437	-0.311	-0.241	-0.197	-0.167
	π/3	(-0.455)	-0.255	-0.177	-0.135	-0.110	-0.092

Table 2 Poisson's ratio ν_Y at the limit value of small deformation

	H/L	1.5	2	2.5	3	3.5	4
λ	π/18	-0.237	-0.327	-0.417	-0.506	-0.596	-0.685
	π/9	-0.449	-0.642	-0.836	-1.030	-1.223	-1.417
	π/6	-0.667	-1	-1.333	1.667	-2	-2.333
	2π/9	-0.939	-1.487	-2.034	-2.582	-3.130	-3.677
	5π/18	(-1.361)	-2.288	-3.215	-4.142	-5.069	-5.996
	π/3	(-2.196)	-3.928	-5.660	-7.392	-9.124	-10.856

NII-Electronic Library Service

The Japan Society of Mechanical Engineers

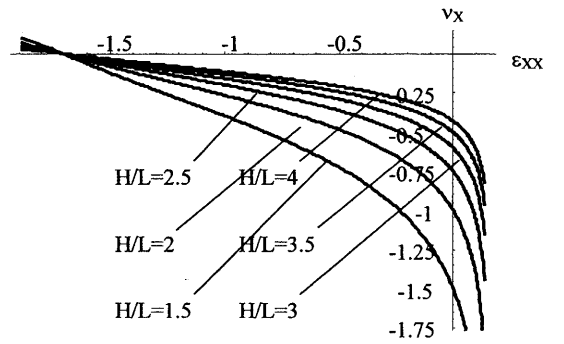

(a) ν_X versus ε_{XX}

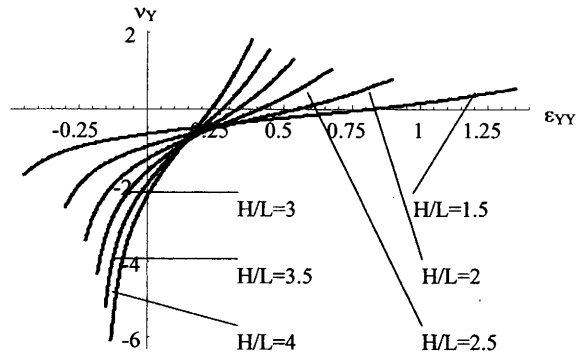

(b) ν_Y versus ε_{YY}

Fig. 8 Effect of H/L on Poisson's ratios for a given value of $\lambda=\pi/6$

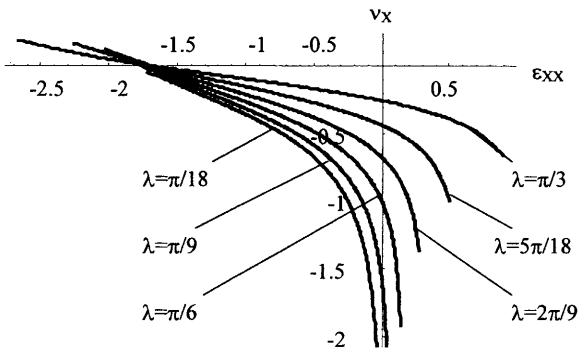

(a) ν_X versus ε_{XX}

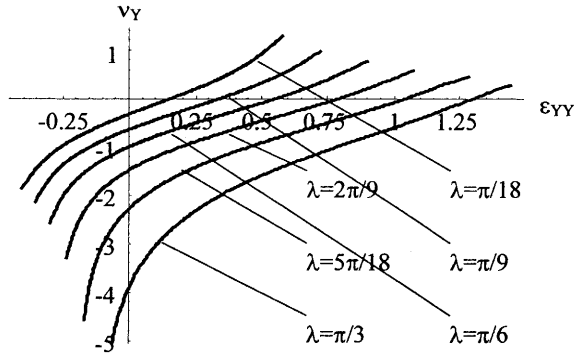

(b) ν_Y versus ε_{YY}

Fig. 9 Effect of λ on Poisson's ratios for a given value of $H/L=2$

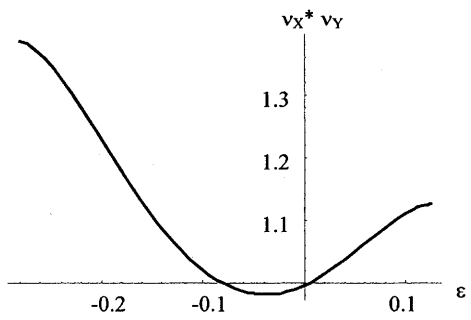

Fig. 10 $\nu_X \cdot \nu_Y$ versus strain for the case study with cell's geometric parameters of $H/L=2$ and $\lambda=\pi/6$

is sufficiently large. The sign of Poisson's ratio changes to positive at a critical strain, which, on the other hand, depends on the value of H/L. Under X-direction compressive remote stress, the sign of Poisson's ratio changes from negative to positive at a strain of about 1.7.

In the effective intervals of tensile ε_X and compressive ε_Y, the variation of $\nu_X \cdot \nu_Y$ with strain is shown in Fig. 10 by a least squares fit. Geometric parameters of the re-entrant cell are: $H/L=2$ and $\lambda=\pi/6$, for the case study. As can be seen, the reciprocal relation for ν_X and ν_Y does not hold when the deformation is large.

4. Conclusions

Nonlinear behavior becomes important when honeycombs are to be used as the load bearing or energy absorption structure, because large deformation often occurs. In this paper, we provide a theoretical approach for evaluating negative Poisson's ratios of re-entrant honeycombs. The prediction of negative Poisson's ratios of these honeycombs is based on the large deflection model, which is also suitable for small flexure and elastic buckling. This large deflection model extends and refines our understanding on negative Poisson's ratios of auxetic honeycombs, giving a complete estimation of negative Poisson's ratios.

It is found that Poisson's ratios of re-entrant honeycombs are not a constant at large deformation, vary significantly with the strain, but converge to the results predicted by the small deformation of flexure at the limit of small strain of this model. At large deformation, the negative Poisson's ratios are different in the case of remote compressive loading and tensile loading. Geometric parameters of the re-entrant cell, i.e., H/L and λ, have very significant effects on the magnitude of the Poisson's ratio. They even change the sign of Poisson's ratio from negative to positive, when this sort of honeycomb bears a Y-direction tensile loading or a X-direction compressive loading under the condition that the deformation is sufficiently large. Orthogonal symmetry of Poisson's ratios occurs for some cell geometric parameters at small deformation, and a re-entrant cell of $H/L=2$ and $\lambda=\pi/6$ is a special one. The reciprocal relation for ν_X and ν_Y is con-

NII-Electronic Library Service

The Japan Society of Mechanical Engineers

served for all geometric parameters when the deformation is small. Neither orthogonal symmetry, nor the reciprocal relation of Poisson's ratios are maintained when the deformation is large.

References

(1) Lakes, R.S., Foam Structures with a Negative Poisson's Ratio, Science, Vol.235 (1987), pp.1038–1040.

(2) Lakes, R.S., Negative Poisson's Ratio Materials, Science, Vol.238 (1987), p.551.

(3) Rothenberg, L., Berlin, A.A. and Bathurst, R.J., Microstructure of Isotropic Materials with Negative Poisson's Ratio, Nature, Vol.354 (1991), pp.470–472.

(4) Evans, K., Nkansah, M.A., Hutchinson, I.J. and Rogers, S.C., Molecular Network Design, Nature, Vol.353 (1991), pp.124–125.

(5) Overaker, D.W., Cuitiño, L.M. and Langrana, N.A., Elastoplastic Micromechanical Modeling of Two-Dimensional Irregular Convex and Nonconvex (Re-entrant) Hexagonal Foams, Transactions of the ASME, Journal of Applied Mechanics, Vol.65 (1998), pp.748–757.

(6) Wang, Y. and Cuitiño, A.M., Three-Dimensional Nonlinear Open-Cell Foams with Large Deformations, Journal of the Mechanics and Physics of Solids, Vol.48 (2000), pp.961–988.

(7) Saiki, I., Terada, K., Ikeda, K. and Hori, M., Appropriate Number of Unit Cells in a Representative Volume Element for Micro-Structural Bifurcation Encountered in a Multi-Scale Modeling, Computer Method in Applied Mechanics and Engineering, Vol.19 (2002), pp.2561–2585.

(8) Ohno, N., Okumura, D. and Noguchi, H., Microscopic Symmetric Bifurcation Condition of Cellular Solids Based on a Homogenization Theory of Finite Deformation, Journal of the Mechanics and Physics of Solids, Vol.50 (2002), pp.1125–1153.

(9) Almgren, R.F., An Isotropic Three-Dimensional Structure with Poisson's Ratio Equal to Minus One, Journal of Elasticity, Vol.15 (1985), p.427.

(10) Wojciechowski, K.W., Two-Dimensional Isotropic System with a Negative Poisson Ratio, Physics Letters A, Vol.137 (1989), pp.60–64.

(11) Wojciechowski, K.W. and Branka, A.C., Negative Poisson Ratio in a Two-Dimensional Isotropic Solid, Physical Review A, Vol.40 (1989), pp.7222–7225.

(12) Warren, W.E. and Kraynik, A.M., Foam Mechanics: The Linear Elastic Response of Two-Dimensional Spatially Periodic Cellular Materials, Mechanics of Materials: An International Journal, Vol.6 (1987), pp.27–37.

(13) Warren, W.E., Kraynik, A.M. and Stone, C.M., A Constitutive Model for Two-Dimensional Non-Linear Elastic Foams, Journal of the Mechanics and Physics of Solids, Vol.37 (1989), pp.717–733.

(14) Wei, G., Negative Poisson's Ratio of Polymeric Networks with Special Microstructures, Journal of Chemical Physics, Vol.96 (1992), pp.3226–3233.

(15) Gibson, L.J. and Ashby, M.F., Cellular Solids: Structure and Properties, 2nd ed., (1997), Cambridge University Press, Cambridge.

(16) Evans, K.E., Tensile Network Microstructures Exhibiting Negative Poisson's Ratios, Journal of Physics D: Applied Physics, Vol.22 (1989), pp.1870–1876.

(17) Evans, K.E., Tailoring the Negative Poisson's Ratio, Chemical Industry, Vol.20 (1990), p.654.

(18) Warren,W.E. and Byskov, A., Three-Fold Symmetry Restrictions on Two-Dimensional Micropolar Materials, European Journal of Mechanics and Solids, Vol.21 (2002), pp.779–792.

(19) Yang, D.U., Lee, S. and Huang, F.Y., Geometric Effect on Micropolar Elastic Honeycomb Structure with Negative Poisson's Ratio Using the Finite Element Method, Finite Elements in Analysis and Design, Vol.39 (2003), pp.187–205.

(20) Sigmund, O., Materials with Prescribed Constitutive Parameters: An Inverse Homogenization Problem, International Journal of Solids and Structure, Vol.31 (1994), pp.2313–2329.

(21) Sigmund, O., A New Class of Extreme Composites, Journal of Mechanics and Physics, Vol.48 (2000), pp.397–428.

(22) Masters, I.G. and Evans, K.E., Models for the Elastic Deformation of Honeycombs, Composite Structure, Vol.35 (1999), pp.403–422.

(23) Lakes, R.S., Deformation Mechanism in Negative Poisson's Ratio Materials: Structure, Journal of Material Science, Vol.26 (1987), pp.2287–2292.

(24) Zhang, J. and Ashby, M.F., Buckling of Honeycombs Under In-Plane Biaxial Stresses, International Journal of Mechanical Sciences, Vol.34 (1992), pp.491–509.

(25) Zhu, H.X. and Mills, N.J., The In-Plane Non-Linear Compression of Regular Honeycombs, International Journal of Solids and Structures, Vol.37 (2000), pp.1931–1949.

NII-Electronic Library Service